Optical trapping and propulsion of red blood cells on waveguide surfaces

Balpreet Singh Ahluwalia,[1,*] Peter McCourt,[2] Thomas Huser,[1,3] and Olav Gaute Hellesø,[1]

[1] *Department of Physics and Technology, University of Tromsø, Tromsø N-9037 Norway*
[2] *Department of Medical Biology, University of Tromsø, Tromsø N-9037 Norway*
[3] *Center for Biophotonics and Department of Internal Medicine, University of California, Davis, Sacramento 95817, California, USA*
**balpreet.singh.ahluwalia@uit.no*

Abstract: We have studied optical trapping and propulsion of red blood cells in the evanescent field of optical waveguides. Cell propulsion is found to be highly dependent on the biological medium and serum proteins the cells are submerged in. Waveguides made of tantalum pentoxide are shown to be efficient for cell propulsion. An optical propulsion velocity of up to 6 µm/s on a waveguide with a width of ~6 µm is reported. Stable optical trapping and propulsion of cells during transverse flow is also reported.

OCIS codes: (170.4520) Optical confinement and manipulation; (230.7370) Waveguides; (130.3120) Integrated optics devices; (140.7010) Laser Trapping; (160.3130) Integrated optics materials.

References and links

1. A. Ashkin, J. M. Dziedzic, and T. Yamane, "Optical trapping and manipulation of single cells using infrared laser beams," Nature **330**(6150), 769–771 (1987).
2. A. Ashkin, "Optical trapping and manipulation of neutral particles using lasers," Proc. Natl. Acad. Sci. U.S.A. **94**(10), 4853–4860 (1997).
3. D. G. Grier, "A revolution in optical manipulation," Nature **424**(6950), 810–816 (2003).
4. P. R. T. Jess, V. Garcés-Chávez, A. C. Riches, C. S. Herrington, and K. Dholakia, "Simultaneous Raman micro-spectroscopy of optically trapped and stacked cells," J. Raman Spectrosc **38**(9), 1082–1088 (2007).
5. K. Ramser, J. Enger, M. Goksör, D. Hanstorp, K. Logg, and M. Käll, "A microfluidic system enabling Raman measurements of the oxygenation cycle in single optically trapped red blood cells," Lab Chip **5**(4), 431–436 (2005).
6. J. El-Ali, P. K. Sorger, and K. F. Jensen, "Cells on chips," Nature **442**(7101), 403–411 (2006).
7. R. Applegate, Jr., J. Squier, T. Vestad, J. Oakey, and D. Marr, "Optical trapping, manipulation, and sorting of cells and colloids in microfluidic systems with diode laser bars," Opt. Express **12**(19), 4390–4398 (2004).
8. S. Kawata, and T. Tani, "Optically driven Mie particles in an evanescent field along a channeled waveguide," Opt. Lett. **21**(21), 1768–1770 (1996).
9. K. Grujic, O. G. Hellesø, J. S. Wilkinson, and J. P. Hole, "Optical propulsion of microspheres along a channel waveguide produced by Cs+ ion-exchange in glass," Opt. Commun. **239**(4-6), 227–235 (2004).
10. A. H. J. Yang, S. D. Moore, B. S. Schmidt, M. Klug, M. Lipson, and D. Erickson, "Optical manipulation of nanoparticles and biomolecules in sub-wavelength slot waveguides," Nature **457**(7225), 71–75 (2009).
11. B. S. Schmidt, A. H. J. Yang, D. Erickson, and M. Lipson, "Optofluidic trapping and transport on solid core waveguides within a microfluidic device," Opt. Express **15**(22), 14322–14334 (2007).
12. S. Gaugiran, S. Gétin, J. M. Fedeli, G. Colas, A. Fuchs, F. Chatelain, and J. Dérouard, "Optical manipulation of microparticles and cells on silicon nitride waveguides," Opt. Express **13**(18), 6956–6963 (2005).
13. D. Néel, S. Gétin, P. Ferret, M. Rosina, J. M. Fedeli, and O. G. Hellesø, "Optical transport of semiconductor nanowires on silicon nitride waveguides," Appl. Phys. Lett. **94**, 253115 (2009).
14. B. S. Ahluwalia, A. Z. Subramanian, O. G. Hellesø, N. M. B. Perney, N. P. Sessions, and J. S. Wilkinson, "Fabrication of submicrometer high refractive index Tantalum Pentoxide waveguides for optical propulsion of microparticles," IEEE Photon. Technol. Lett. **21**(19), 1408–1410 (2009).
15. B. S. Ahluwalia, O. G. Hellesø, A. Z. Subramanian, J. Chen, J. S. Wilkinson, and X. Chen, "Integrated platform based on high refractive index contrast waveguide for optical guiding and sorting," Proc. SPIE **7613**, 76130R (2010).
16. H. Jaising, K. Grujić, and O. G. H. Tomita, "Simulations and Velocity Measurements for a Microparticle in an Evanescent Field," Opt. Rev. **12**(1), 4–6 (2005).
17. H. Y. Jaising, and O. G. Hellesø, "Radiation forces on a Mie particle in the evanescent field of an optical waveguide," Opt. Commun. **246**(4-6), 373–383 (2005).

#129596 - $15.00 USD Received 14 Jun 2010; revised 2 Aug 2010; accepted 3 Aug 2010; published 21 Sep 2010

18. S. Gaugiran, S. Gétin, J. M. Fedeli, and J. Derouard, "Polarization and particle size dependence of radiative forces on small metallic particles in evanescent optical fields. Evidences for either repulsive or attractive gradient forces," Opt. Express **15**(13), 8146–8156 (2007).
19. D. Néel, S. Gétin, P. Ferret, M. Rosina, J. M. Fedeli, and O. G. Hellesø, "Optical transport of semiconductor nanowires on silicon nitride waveguides," Appl. Phys. Lett. **94**, 253115 (2009).
20. G. Sagvolden, I. Giaever, E. O. Pettersen, and J. Feder, "Cell adhesion force microscopy," Proc. Natl. Acad. Sci. U.S.A. **96**(2), 471–476 (1999).
21. J. N. George, R. I. Weed, and C. F. Reed, "Adhesion of human erythrocytes to glass: the nature of the interaction and the effect of serum and plasma," J. Cell. Physiol. **77**(1), 51–59 (1971).
22. G. W. Francis, L. R. Fisher, R. A. Gamble, and D. Gingell, "Direct measurement of cell detachment force on single cells using a new electromechanical method," J. Cell Sci. **87**(Pt 4), 519–523 (1987).
23. E. Evans, and Y. C. Fung, "Improved measurements of the erythrocyte geometry," Microvasc. Res. **4**(4), 335–347 (1972).
24. S. Hénon, G. Lenormand, A. Richert, and F. Gallet, "A new determination of the shear modulus of the human erythrocyte membrane using optical tweezers," Biophys. J. **76**(2), 1145–1151 (1999).
25. M. Dao, C. T. Lim, and S. Suresh, "Mechanics of the human red blood cell deformed by optical tweezers," J. Mech. Phys. Solids **51**(11-12), 2259–2280 (2003).
26. A. Ghosh, S. Sinha, J. A. Dharmadhikari, S. Roy, A. K. Dharmadhikari, J. Samuel, S. Sharma, and D. Mathur, "Euler buckling-induced folding and rotation of red blood cells in an optical trap," Phys. Biol. **3**(1), 67–73 (2006).
27. S. C. Grover, R. C. Gauthier, and A. G. Skirtach, "Analysis of the behaviour of erythrocytes in an optical trapping system," Opt. Express **7**(13), 533–539 (2000).
28. D. Psaltis, S. R. Quake, and C. Yang, "Developing optofluidic technology through the fusion of microfluidics and optics," Nature **442**(7101), 381–386 (2006).
29. M. Pelton, K. Ladavac, and D. G. Grier, "Transport and fractionation in periodic potential-energy landscapes," Phys. Rev. E Stat. Nonlin. Soft Matter Phys. **70**(3 Pt 1), 031108 (2004).
30. K. Ladavac, K. Kasza, and D. G. Grier, "Sorting mesoscopic objects with periodic potential landscapes: optical fractionation," Phys. Rev. E Stat. Nonlin. Soft Matter Phys. **70**, 010901 (2004).
31. K. Grujic, and O. G. Hellesø, "Dielectric microsphere manipulation and chain assembly by counter-propagating waves in a channel waveguide," Opt. Express **15**(10), 6470–6477 (2007).
32. S. Rao, Š. Bálint, B. Cossins, V. Guallar, and D. Petrov, "Raman study of mechanically induced oxygenation state transition of red blood cells using optical tweezers," Biophys. J. **96**(1), 209–216 (2009).
33. B. Hansen, J. Melkko, and B. Smedsrød, "Serum is a rich source of ligands for the scavenger receptor of hepatic sinusoidal endothelial cells," Mol. Cell. Biochem. **229**(1-2), 63–72 (2002).
34. K. Grujic, O. Hellesø, J. Hole, and J. Wilkinson, "Sorting of polystyrene microspheres using a Y-branched optical waveguide," Opt. Express **13**(1), 1–7 (2005).

1. Introduction

Cells are the smallest living structures in the body acting as a building unit in tissues. Cellular processes and inter-cellular interactions lead to the basic functions of organs. Optical techniques like laser tweezers can be used to investigate cellular level processes and cell-cell interaction [1–4]. There, the optical forces arising from a focused laser beam are used to trap and manipulate cells at single cell level. Integrated lab-on-a-chip and micro-fluidic techniques have been developed for rapidly manipulating large number of cells [5–7].

In conventional optical tweezers, the focused laser beam generates a high intensity gradient near the focal spot. The optical gradient forces dominate over scattering forces in the focal region. By maneuvering the location of a focal spot the trap position can be steered. Thus, optical tweezers allow trapping of cells in three dimensions at any desired location, usually away from surfaces [4].

The evanescent field surrounding an optical waveguide, however, can also be used for optical trapping [8–19]. The decay length of the evanescent field is within 250 nm from the waveguide surface [9,15]. Consequently, targets are trapped close to the surface [8–19]. In waveguide trapping, the gradient forces attract the target to the waveguide and the radiation forces propel it along the waveguide. The waveguides can be designed to trap different sizes and types of particles, and to trap single particles or several particles in parallel. Moreover, trapping on optical waveguides can also be integrated with lab-on-a-chip systems [13].

Optical propulsion of polystyrene micro-particles, gold nano-particles and nano-rods on waveguide surfaces has been comprehensively reported [8–19]. However, so far only one example of trapping of cells on waveguides has been reported [12]. There are two major challenges for efficient trapping and propulsion of cells on a waveguide surface: cellular adhesion to surfaces and the rather small difference in refractive index between cells and

#129596 - $15.00 USD Received 14 Jun 2010; revised 2 Aug 2010; accepted 3 Aug 2010; published 21 Sep 2010

water. Adherent cells readily (and rapidly) stick to each other and a large number of surfaces [20] as they are naturally programmed to perform common cellular activities, such as mitosis, cell-cell interactions and cell motility on a substrate. Even non-adherent cells, e.g. red blood cells, in some cases stick to surfaces, presumably due to electrostatic forces arising from salt ions in the medium [21,22]. As we will show here, surface forces can dominate over optical forces, inhibiting optical propulsion of cells. The second challenge is the refractive index of cells, which is close to that of water. Most cells have a refractive index of 1.35-1.4, compared to 1.33 for water. Since the optical forces depend on the refractive index contrast between the target and the medium, the forces are smaller than the cells for e.g. polystyrene, glass and gold particles of similar size. To overcome this limitation, higher intensities must be used, which can be obtained with a small waveguide core with a high refractive index.

Here, a systematic study of optical propulsion of fixed and live red blood cells (RBCs), on a waveguide surface is reported. Comparisons are made for waveguides fabricated using two different methods; diffusion of Cesium-ions into glass, and deposition of Ta_2O_5 on silica. The propulsion velocity of RBCs is shown to depend on the waveguide width. Waveguide cell propulsion in different cell culture media is investigated. Finally, it is shown that RBCs can be trapped and propelled in a transverse flow.

2. Materials and Methods

2.1 Cell preparation

Red blood cells (RBCs) are typically disk-shaped, with a diameter between 6 and 8 μm and a thickness of approximately 2 μm. The refractive index of red blood cells is around 1.38 [23]. Their shape depends on the environment, and can also be spherical. Fixed RBCs are mostly spherical [23].

Fresh blood samples were drawn from healthy donors (6-10 ml) by venipuncture into EDTA-containing (ethylenediaminetetraacetic acid) tubes, which chelate calcium to prevent clotting. The blood sample wss mixed with phosphate buffered saline solution (PBS) and centrifuged at 600g for 10 minutes. This accumulates RBC pellets at the bottom of the test tube. The supernatant containing white blood cells and plasma was carefully decanted. This process is repeated three times in PBS to remove most of the plasma and white blood cells. For live RBC experiments the samples are stored in PBS solution and were used within two hours. For fixed RBC experiments, the RBC pellet was resuspended in 4% paraformaldehyde and 96% PBS. We used fixed RBC mostly for optimization experiments, i.e. finding optimal waveguide materials and suspension media. The results shown in section 3 are obtained with fixed RBCs and the results in sections 4-5 are performed with live RBCs.

2.2 Experimental set-up

The experimental apparatus for cell propulsion on waveguides is shown in Fig. 1. The laser is a 5 W single-mode Ytterbium fiber laser, with 1070 nm wavelength. Light was coupled into the waveguide by an objective lens (80X, 0.9 N.A, NIR Nachet). The objective was positioned with a piezoelectric translation stage with ~10 nm step size. The waveguide chip was continuously held by vacuum suction to avoid any mechanical drift with time. The output light from the waveguide was collected by a 40X objective lens. A microscope with a long working distance 20X objective lens and a CCD camera was employed to capture images of the waveguide and cells from above. The cell propulsion velocity was measured by capturing real-time video footage of the experiment. The video data was analyzed to measure the distance traveled by the cells with respect to time.

#129596 - $15.00 USD Received 14 Jun 2010; revised 2 Aug 2010; accepted 3 Aug 2010; published 21 Sep 2010

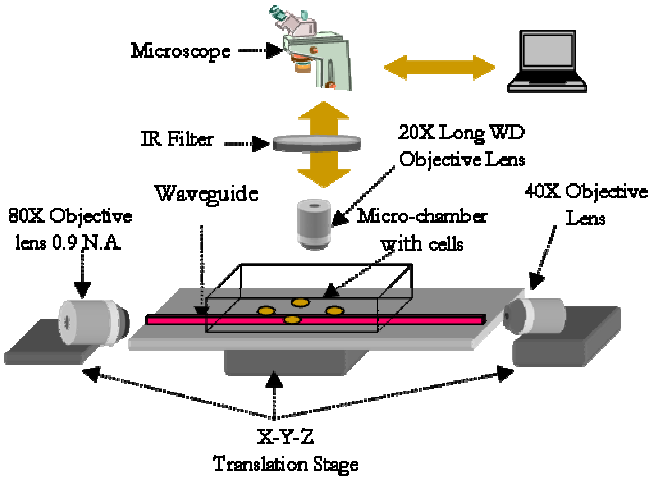

Fig. 1. Schematic diagram of the experimental set-up for optical propulsion of cells on waveguides.

2.3 Optical waveguides

High intensity in the evanescent field is crucial for efficient cell propulsion on waveguides. The conventional waveguide materials used for propulsion of polystyrene micro-particles and gold nano-particles can be broadly classified according to refractive index of core relative to substrate: a) low Δn ($\leq$0.04) Cs^+ or K^+ ion-exchange waveguides [8,9] and b) high Δn waveguides like silicon nitride (Si_3N_4, Δn ~0.52) [12,13] and Ta_2O_5 waveguides (Δn ~0.65) [14,15].

Simulations can be used to optimize the waveguide parameters for maximum optical forces. The optical forces on a particle in an evanescent field depend on the optical properties of the particle and on the strength of the evanescent field. A two-dimensional simulation (e.g. with finite element method) can be used to optimize the waveguide parameters for maximum evanescent field. For Ta_2O_5 waveguides we found that 200nm thickness was optimal (at 1070nm) [14,15]. Thinner waveguides will approach cut-off and thicker waveguides will have less evanescent field. To find the optical forces on a particle using the Maxwell-stress tensor, three-dimensional models are necessary. Mie theory can be used to simulate optical forces on spherical microparticles [16,17]. Rayleigh theory can be employed to simulate optical forces on nano-particles [12]. Finite element method can be used to simulate non-spherical particles (such as nano-rods) [19]. RBCs are disk-shaped with a diameter of 7-8 μm. Simulation of such structures employing finite element method increases the computational time significantly and has not been explored yet.

It has recently been shown experimentally that Ta_2O_5 waveguides are more efficient than Si_3N_4 waveguides for propelling polystyrene micro-particles [14]. Similarly, Cs^+ ion-exchange waveguides with higher refractive index contrast (Δn = 0.03) are more efficient for particle propelling than K^+ ion-exchanged waveguides (Δn = 0.01) [9]. Based on this, we chose to use Ta_2O_5 and Cs^+ ion-exchanged waveguides for this work on cell propulsion. The Ta_2O_5 waveguides were made by magnetron sputtering, photolithography and ion-beam milling, see [14,15] for details. The Cs^+ waveguides were made by evaporation of an aluminium mask, photolithography and thermal ion-exchange (Cs^+ exchanged with K^+ or Na^+ in the glass) [9].

Both low and high Δn waveguide materials have advantages and disadvantages. The surface intensity of high Δn waveguides (Ta_2O_5) is larger than for low Δn waveguides (Cs^+ ion-exchange) for the same guided power [12,14]. However, for the same input laser power and using an objective for input coupling, more light can be coupled into a Cs^+ ion-exchanged waveguide than in a Ta_2O_5 waveguide. The ion-exchanged and Ta_2O_5 waveguides are around 1 μm and 200 nm thick respectively. The insertion losses of ion-exchanged waveguides are

#129596 - $15.00 USD Received 14 Jun 2010; revised 2 Aug 2010; accepted 3 Aug 2010; published 21 Sep 2010

~6-8 dB [8] as compared to 8-12 dB for Ta_2O_5 waveguides discussed below. Thus, in the next section, both waveguide materials are tested to determine their efficiency for cell propulsion.

The insertion loss of Ta_2O_5 waveguides (2.5 cm long and 200 nm thick) as a function of width is shown in Table 1. The insertion loss of a waveguide is calculated by measuring the input and the output power. The insertion loss comprises both coupling and propagation losses. The propagation loss was determined by the cut-back method. Finally, the value of coupling loss was obtained by subtracting propagation loss from the insertion loss. Further details on loss measurement can be found elsewhere [14,15]. Narrow waveguides (2-4 μm) have higher losses compared to wider waveguides (5-10 μm). This is mainly due to high coupling losses and sidewall scattering losses for the narrow waveguides [14,15]. Thus, for a given input power, more light is coupled (guided) into the wide waveguides (≥ 5 μm) than the narrow waveguides (≤ 4 μm). This influences the propulsion velocity of cells on waveguides of different widths as highlighted in section 3.1.

The propulsion velocities of RBCs in section 3 and 4 are plotted as a function of input power. The output power depends on number of trapped cells along the length of the waveguide. The output power also varies for the different width of the waveguides due to varying insertion losses as shown in Table 1. In our experience, the output power tends to fluctuate and it is difficult to keep it constant during experiment. It is thus more practical to plot propulsion velocity as a function of input power.

Table 1. Insertion loss on 2.5 cm long Ta_2O_5 waveguide

Width of waveguide	8 - 10 μm	5 – 7 μm	2 – 4 μm
Insertion Loss	8 dB	9 dB	12 dB

3. Optical propulsion of fixed RBC

3.1 Choice of waveguide material

Conventional optical tweezers have being employed to trap and manipulate red blood cells [24–27]. The original paper on optical trapping of RBCs was published in 1987 by Ashkin *et. al*. Here, we study optical trapping and propulsion of RBCs on optical waveguides (Ta_2O_5 and Cs^+ ion-exchange). A 40X coupling objective lens was employed for Cs + ion-exchange waveguides and an 80X coupling objective lens was used for Ta_2O_5 waveguides. The rest of the experimental set-up was similar to that shown in Fig. 1. The optical propulsion velocity of the fixed RBC on Ta_2O_5 and Cs^+ ion-exchange waveguide materials is shown in Fig. 2. The suspension medium for the cells was water, and the width of the waveguides was ~10 μm. The input power was kept constant at 800 mW for both waveguides. The guided power was estimated to be 20 mW for the Ta_2O_5 waveguide and 150 mW for the Cs^+ ion-exchange waveguide. The guided power was approximated from the output power after compensating the out-coupling loss. Ta_2O_5 waveguides were found to be much more efficient for cell propulsion than Cs^+ ion-exchange waveguides, as shown in Fig. 2. The optical propulsion velocity of a fixed RBC was five times higher on a Ta_2O_5 waveguide than on a Cs^+ ion-exchange waveguide. Thus, for the remaining experiments in this paper we used Ta_2O_5 waveguides for cell propulsion.

#129596 - $15.00 USD Received 14 Jun 2010; revised 2 Aug 2010; accepted 3 Aug 2010; published 21 Sep 2010

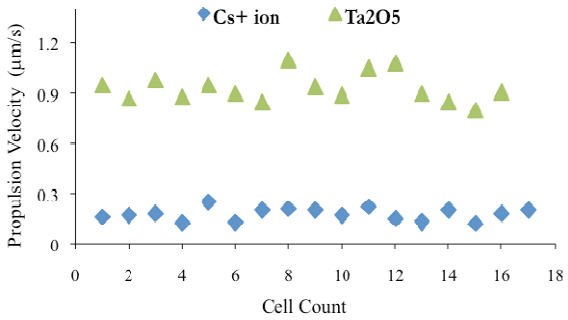

Fig. 2. Comparison of cell propulsion velocity on a Cs^+ ion exchange and a Ta_2O_5 waveguide. Input power is 800 mW and width of waveguides ~10 μm.

3.2 Choice of suspension medium

Cells must ideally be propelled in a medium in which they can stay healthy and alive. Cells will rupture (in hypotonic medium) or shrink (in hypertonic medium) if not kept under isotonic conditions. We have investigated waveguide cell propulsion in the following cell culturing media: a) phosphate buffered saline solution (PBS), b) Hepes (4-(2-hydroxyethyl)-1-piperazineethanesulfonic acid) 20 mM concentration, and c) 0.25 M isotonic sucrose solution. We have also studied how addition of different serum proteins and whole serum influenced cell propulsion. The serum proteins studied were a) human serum albumin (HSA), b) bovine serum albumin (BSA) and c) fetal calf serum (FCS). Table 2 summarizes the results of optical propulsion of fixed RBC in these media and serum proteins/serum. Interestingly, we were only able to successfully propel the cells in water and 0.25 M isotonic sucrose medium. Addition of BSA and FCS resulted in cessation of cell propulsion in these media. The experiments with addition of HSA showed cell propulsion a few times, but were not repeatable and thus inconclusive. The cells were not propelled in PBS and Hepes media neither with nor without serum.

We hypothesize that the presence of salt ions in PBS and Hepes media are the reason for cells adhering to the waveguide surfaces. In waveguide trapping, the optical forces are dependant on the refractive index contrast between the target and the medium (Δn). The optical trapping forces on polystyrene micro-particles (Δn = 0.26) are in the range of pN [16,17]. For biological cells with Δn = 0.05, these forces will be even smaller. The adhesive forces between RBC and the surfaces in physiological saline medium (PBS with sera) have been previously characterized [21,22]. In PBS medium a centrifugal force of 0.5-0.15 nN was found insufficient to move stuck RBC from a surface [21,22]. The cell adhesive force in PBS is thus two orders of magnitude higher than the optical trapping forces generated in a waveguide. This provides the most likely reason for causing cells to stick to waveguide surfaces in media with high salt concentration. It is possible to explore waveguide surface treatment and decreasing ionic strength of the medium to alleviate the sticking problems in PBS. Surface treatment has not been explored in the present studies.

Next, optical propulsion velocities in water and isotonic sucrose media were compared. Figure 3 shows cell propulsion velocities as a function of input power in these two media. The cell propulsion velocity was found to be linear with the input power. The cells generally propelled with higher velocity in water than the sucrose medium. However, cells will lyse in pure water due to the difference in the osmotic pressure between the cell and the surrounding water. An isotonic medium is essential for a cell to maintain their structure. Therefore, for all the remaining experiments discussed below an isotonic sucrose medium was employed for cell propulsion.

#129596 - $15.00 USD Received 14 Jun 2010; revised 2 Aug 2010; accepted 3 Aug 2010; published 21 Sep 2010

Table 2. Optical propulsion of RBC in different media and sera

Medium	Serum-free	HSA 5% by volume	BSA 5% by weight	FCS 10% by volume
Water	Yes	Inconclusive	No	No
Isotonic sucrose	Yes	Inconclusive	No	No
PBS	No	No	No	No
HEPES	No	No	No	No

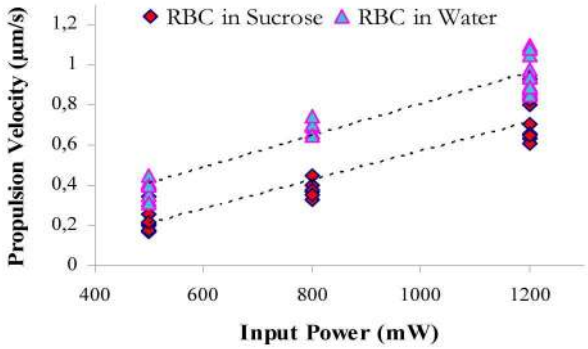

Fig. 3. Comparison of optical propulsion velocity of a cell in water and isotonic sucrose media as a function of input power. Ta_2O_5 waveguide of width ~10 µm was used.

4. Optical propulsion of Live RBCs

Live RBCs were optically trapped using the optimized waveguide material (Ta_2O_5) and medium (isotonic sucrose). We have recently shown that for a given input power, the propulsion velocity of a polystyrene micro-particle varies with the waveguide width [15]. The study found that the width of a waveguide must be carefully chosen for differently sized micro-particles to impart the largest optical force. Thus, optical propulsion velocities of cells were investigated as a function of input power and waveguide width, as shown in Fig. 4. For each width, the propulsion velocities of cells at specific input powers exhibit a wide spread. The size of RBCs varies between 6 and 8 µm, which could lead to a variation of propulsion velocity at a given input power.

As shown in Fig. 4, a 6 µm wide waveguide trapped and propelled cells with a maximum velocity of ~6 µm/s. Light is confined less tightly inside a 10 µm wide waveguide resulting in a weaker intensity near the surface and slow cell propulsion. Furthermore, propelling a cell (~7 µm diameter) over a 10 µm wide waveguide implies that the cell does not interact with the entire evanescent field present. Even though light is confined most tightly in a 3 µm wide waveguide, it has higher insertion losses (as shown in Table 1). Consequently, at a given input power less light is guided in a 3 µm wide waveguides, resulting in slower cell propulsion than on a 6 µm wide waveguide. Thus, to impart higher optical forces for efficient cell propulsion, a waveguide of optimum width must be chosen (6 µm in our case).

Optical propulsion of live RBCs on a 6 µm wide waveguide is depicted in Fig. 5. The interaction between the evanescent field and the cell generates gradient and radiation forces. The cells are laterally trapped on top of a waveguide surface by the gradient force. The radiation force propels the trapped cell along the waveguide. It is worth highlighting that the actual guided power was small, even though a high input power was employed in the experiments. Due to high coupling losses the maximum guided power was ~60 mW for a 6 µm wide waveguide when the cell propulsion velocity was 6 µm/s. From simulations it was found that ~10% of the total guided power will be present in the evanescent field for the chosen waveguide material and dimension.

#129596 - $15.00 USD Received 14 Jun 2010; revised 2 Aug 2010; accepted 3 Aug 2010; published 21 Sep 2010

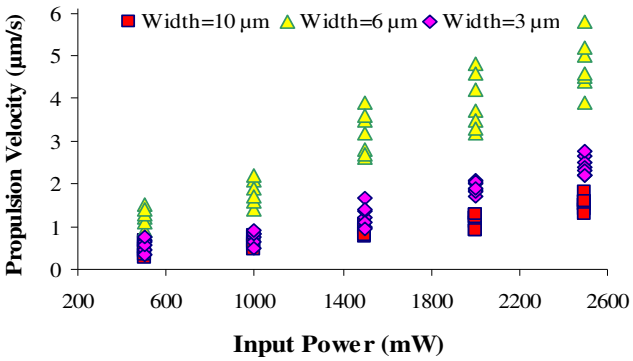

Fig. 4. Optical propulsion velocities of live RBCs as a function of input power and the width of waveguides.

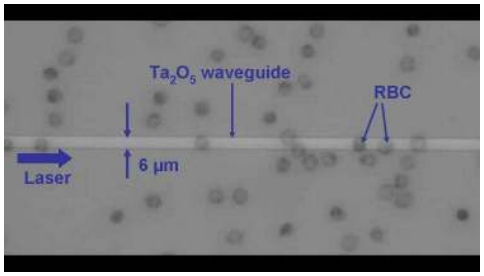

Fig. 5. (Media 1) Optical propulsion of live RBCs on a 6µm wide Ta_2O_5 waveguide.

5. Optical propulsion of cells in the presence of transverse flow

Opto-fluidics combines the advantages of micro-fluidics and optics on a common platform [28]. Integration of micro-fluidics with cell propulsion on waveguides is imperative for efficient and rapid cell manipulation, as a larger number of cells can be transported faster with flow than with optical methods. On the other hand, it is easier to precisely manipulate single cells with optical methods. The two methods can be tailored to sort cells based on optical fractionation techniques [29,30]. Optofluidic trapping on a waveguide surface has previously only been reported for polystyrene microparticles [11].

Figure 6 shows optical trapping and propulsion of cells in the presence of a transverse flow. A 6 µm wide waveguide was used, as this width provided the highest velocity based on our findings in Fig. 4. The total size of the microchip employed in our experiments was 200 µm in height and 1 mm in width. The microchip was made in PDMS (Polydimethylsiloxane), due to its optical transparent and chemically inert properties. The input power used in the experiment was 1 W. The transverse flow rate of the RBCs was ~1µm/s. The fluid flow delivers the cells close to the waveguide surface, where they are trapped and propelled along the propagation direction of light. A 4X objective lens is employed for imaging to cover a large field-of-view in this experiment. As the laser is switched-off, the trapped cells are released and are drawn away by the flow.

#129596 - $15.00 USD Received 14 Jun 2010; revised 2 Aug 2010; accepted 3 Aug 2010; published 21 Sep 2010

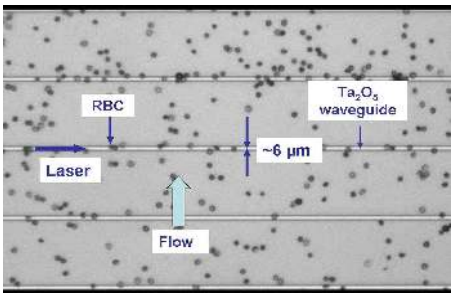

Fig. 6. (Media 2) Optical trapping and propulsion of RBC in the presence of transverse flow.

6. Conclusions

Optical trapping and propulsion of live red blood cells in the evanescent field of an optical waveguide is reported. It is shown that Ta_2O_5, due to its high refractive index contrast, provides an ideal platform for waveguide cell propulsion. Waveguides with a width of ~6 µm were found to propel cells with the highest velocities, 6 µm/s, which is significantly higher than previously reported [12]. Increasing the power in the waveguide, e.g. by decreasing coupling losses, would further increase the propulsion velocity. The velocities demonstrated are compatible with the field-of-view used in high-resolution microscopy. The method may be used to move a single cell to a given position in the field-of-view, hold the cell using counter-propagating beams [31] and study it with high-resolution techniques e.g. confocal-, fluorescence- or Raman-microscopy [32].

Waveguide trapping and propulsion of cells in the presence of a transverse flow is reported. This demonstrates that the cells are stably trapped also transversally relative to the waveguide. Microfluidics can move more cells faster than optical methods, while it is possible to manipulate single cells with optical methods. Combining the two methods in an optofluidics system is thus advantageous, e.g. for the envisioned application in microscopy and for Lab-on-a-Chip applications.

Most cell friendly media, such as sera and PBS, are found to be incompatible with optical trapping on a waveguide surface. However, cells were successfully trapped and propelled in isotonic sucrose, which stabilizes the osmotic pressure of the cells. Surface treatment of the waveguides may reduce the cell adhesion in sera and PBS, and thus make optical propulsion possible in these media. It is, however, important to note that sera, which is derived from clotted blood, is not a natural media for cells in vivo. Serum is full of ligands for scavenger receptors, which bind negatively charged proteins. Therefore, plasma may be a more appropriate media to study in future [33].

Waveguide cell propulsion is influenced by cell parameters like refractive index, cell membrane thickness, shape and size of the cells. It is feasible to sort cells based on different propulsion velocities (for cells with different parameters) and by implementing waveguide designs like a Y-junction [34].

Acknowledgments

The authors thank Pål Løvhaugen, James Wilkinson, and Ananth Subramanian for their help. This work is supported by the Research Council of Norway under the FRINAT-programme.

#129596 - $15.00 USD Received 14 Jun 2010; revised 2 Aug 2010; accepted 3 Aug 2010; published 21 Sep 2010